APPLICATION OF 2D RECURSIVE FILTER FOR ATTENUATING FOOTPRINT NOISE IN SEISMIC DATA PROCESSING

REZA MOHEBIAN and MOHAMMAD ALI RIAHI

Institute of Geophysics, University of Tehran, P.O. Box 14115-6466, Tehran, Iran.
mariahi@ut.ac.ir

(Received September 7, 2018; revised version accepted July 8, 2019)

ABSTRACT

Mohebian, R. and Riahi, M.A., 2019. Application of 2D recursive filter for attenuating footprint noise in seismic data processing. *Journal of Seismic Exploration*, 28: 577-591.

The footprint noise usually appears on 3D seismic data either due to insufficient sampling during acquisition or incorrect/unsuitable processing. The presence of this noise conceals the geological information conveyed by the seismic data and appropriate imaging of the underlying structure leads towards attenuating such noises. Ideally, the seismic footprint noise attenuation should be included within the seismic data processing steps; however, such a measure is not usually taken into the conventional processing sequence. For this purpose, an extra effort is required to be done in order to better understand the nature of the footprint noise which itself is dependent upon the geometry of acquisition and depth of the events. In this paper, a method based on applying the 2D recursive filter for footprint noise attenuation has been presented as a step within the seismic data processing sequence. This filter is different and superior to the conventional Cooley-Tukey filter and can significantly increase the seismic data quality.

KEY WORDS: footprint noise, 2D recursive filter, low pass filter, processing.

0963-0651/19/$5.00

INTRODUCTION

Acquisition footprint is a field noise that appears on 3D seismic amplitude slices or horizons as an interwoven linear crosshatching parallel to source lines and receiver lines. It is, for the most part, an expression of inadequate acquisition geometry, result in insufficient sampling of the seismic wave field (aliasing) and irregularities in the offset and azimuth distributions, particularly parallel to the cross-lines.

Sometimes source-generated noise and incorrect processing (for example inappropriate/erroneous residual NMO due to erroneous velocity picks, incomplete migration, or other systematic errors) can accentuate the footprint. This noise can interfere with the mapping of stratigraphic features and fault patterns, posing a challenge to seismic interpreters.

A remarkable study on the attenuation of the footprint noise on 3D seismic data was conducted by Meunier and Belissent (1993). Their remedy to the problem was to reduce the amplitude and phase perturbations by applying a geometry-based filter on the poststack seismic data. Then, Gulunay (1999) proposed a filtering method of matching corrugated wave number based on frequency slices. Drummond et al. (2000) presented the application of corrugated wavenumber filtering based on time slices; because their method for filter extraction was not consistent with the data and the sound patterns were different with respect to time. Therefore, they suggested the application of the adaptive noise reduction.

The final time slice filtering in 3D seismic data to reduce the footprint noise was presented by Soubaras (2002). Karagul and Crawford (2003) showed noticeable results associated with a complex set of data using the method of Soubaras (2002).

Al-Bannagi et al. (2005) presented singular value decomposition (SVD) filtering for time slices, where the attenuation of the footprint noise and the random noise are performed in a single stage by selecting singular values. Gulunay et al. (2006) presented the footprint noise attenuation in 3D land seismic data. Other authors such as Marfurt et al. (1998), Rost and Thomas (2002), Gibbons and Ringdal (2006), Ben-Zion et al. (2015), de Groot and Hedlin (2015), Li et al. (2015), Riahi and Gerstoft (2015), Soleymani et al. (2010), Inbal et al. (2016), Li and Yao (2016) Riahi and Gerstoft (2016), Alali et al. (2016) have also studied and practiced the noise suppression of seismic data.

In this paper, using a 2D recursive filter of Pupeikis (2015), the footprints noise attenuation scheme is applied to a 3D seismic data of one of the hydrocarbon fields in southern Iran, and the results are presented and discussed.

METHODOLOGY

2D conventional Cooley-Tukey filter

One of the methods used to attenuate the footprint noise is the use of the 2D conventional Cooley-Tukey (1965) filter (FFT). The following equation is used by Sahai and Sufi (2006) for such a purpose:

$$X(k_1,k_2) \equiv X(\frac{2\pi k_1}{N_1},\frac{2\pi k_2}{N_2}) = \left[\sum_{n_1=0}^{N_1-1}\left[\sum_{n_2=0}^{N_2-1} x(n_1,n_2)e^{-\frac{j\,2\pi n_2 k_2}{N_2}}\right]e^{-\frac{j\,2\pi n_1 k_1}{N_1}}\right] \quad (1)$$

having $0 \le k_1 \le N_1 - 1, 0 \le K_2 \le N_2 - 1$. Pupeikis (2015) states that the 2D conventional Cooley-Tukey (FFT) filter is not appropriate for signals that are time-varying such as seismic signals and therefore the 2D recursive FFT filter was introduced to fill this gap. The algorithm of the filter is as follows:

$$\begin{bmatrix} X^{(1)}(K_1,0) \\ X^{(1)}(K_1,1) \\ \dots \\ X^{(1)}(K_1,N-1) \end{bmatrix} = \begin{bmatrix} X^{(0)}(K_1,0) \\ X^{(0)}(K_1,1) \\ \dots \\ X^{(0)}(K_1,N-1) \end{bmatrix} + \left[\sum_{n_1=0}^{N-1}\left[\sum_{n_2=0}^{N-1}\Delta^{(1)}x(l_1,l_2)W_N^{n_2k_2}\right]W_N^{n_1k_1}\right] = \begin{bmatrix} X^{(0)}(K_1,0) \\ X^{(0)}(K_1,1) \\ \dots \\ X^{(0)}(K_1,N-1) \end{bmatrix} + W\,\Delta^{(1)}x(l_1,l_2)W. \quad (2)$$

where $(X^{(0)}(K_1,0)X^{(0)}(K_1,1)...X^{(0)}(K_1,N-1))^T, 0 \le K_1 \le N_1 - 1$. In this method, iteration for each sample in the signal, as in the conventional 2D Cooley-Tukey filter, is discarded. It also significantly reduces the complex operation of the multiplication (CMAD) for a variable-frequency signal (Pupeikis, 2015).

Let us explain a short summary of recursive formulas for recalculating some basic 2D DFT spectrum samples from Pupeikis (2015). Based on this research we have:

$$X(k_1,k_2), 0 \le k_1 \le N_1 - 1, 0 \le k_2 \le N_2 - 1$$

after a new sample appears in the known data matrix of a 2D signal

$$\{x(n_1,n_2)\}, 0 \le n_1 \le N_1 - 1, 0 \le n_2 \le N_2 - 1 \ ,$$

while the respective previous one vanishes. Then, eq. (2) can be rewritten as follows:

$$\mathrm{X}_{old}(k_1,k_2)=\sum_{n_1=0}^{N_1-1}[\sum_{n_2=0}^{N_2-1} x_{old}(n_1,n_2)W_{N_2}^{n_2k_2}]\mathrm{W}_{N_1}^{n_1k_1}=$$

$$\sum_{n_2=0}^{N_2-1} G(n_1,k_2)W_{N_1}^{n_1k_1},$$

if we assume that the new sensor's observation does not change the spectrum considerably or

$$\mathrm{X}_{new}(k_1,k_2)=\sum_{n_1=0}^{N_1-1}[\sum_{n_2=0}^{L-1} x_{old}(n_1,n_2)W_{N_2}^{n_2k_2} +$$

$$\sum_{n_2=L}^{N_2-1} x_{new}(n_1,n_2)W_{N_2}^{n_2k_2}]\mathrm{W}_{N_1}^{n_1k_1},$$

The seismic data is recorded in three dimensions and therefore it has three coordinates: x, y, and t. Subtracting the spectrum values, given in both equations, we obtain the 2D relationship of the form:

$$\begin{bmatrix} X_{new}(k_1,0) \\ X_{new}(k_1,1) \\ \cdots \\ X_{new}(k_1,N_2-1)] \end{bmatrix} - \begin{bmatrix} X_{old}(k_1,0) \\ X_{old}(k_1,1) \\ \cdots \\ X_{old}(k_1,N_2-1)] \end{bmatrix} =$$

$$\sum_{n_1=0}^{N_1-1}[\sum_{n_2=0}^{N_2-1} \triangle x(l_1,l_2)W_{N_2}^{n_2k_2}]\mathrm{W}_{N_1}^{n_1k_1},$$

The mentioned equation can also be rewritten in the recursive form as follows:

$$\begin{bmatrix} X^{(t+1)}(k_1,0) \\ X^{(t+1)}(k_1,1) \\ \cdots \\ X^{(t+1)}(k_1,N_2-1)] \end{bmatrix} = \begin{bmatrix} X^{(t)}(k_1,0) \\ X^{(t)}(k_1,1) \\ \cdots \\ X^{(t)}(k_1,N_2-1)] \end{bmatrix} +$$

$$\left\{ \sum_{n_1=0}^{N_1-1}[\sum_{n_2=0}^{N_2-1} \triangle^{(t+1)} x(l_1,l_2)W_{N_2}^{n_2k_2}]\mathrm{W}_{N_1}^{n_1k_1} \right\}$$

the spectrum formulas are computed with help of Matlab. The Matlab script is shown in the Appendix.

Fig. 1 is a depiction of the seismic data under study. The Field acquisition parameters are as follow:

Recording Parameters	
Type of Instrument:	408XL
No. of Channels:	2683
No. of Used Channels:	2680
No. of Aux. Channels:	3
Recording Length:	7s
Sample Rate:	2ms
Pre-amplifier Gain:	12dB
Low-cut Frequency:	OUT
High-cut Frequency:	0.8 Nyquistminphase
Polarity of Instrument:	Negative
Geometry	
Observing Type:	3D
No. of Receiving Lilnes:	12
Receiving Line Interval:	360m
No. of Traces:	2688
Trace Per Line:	224
Trace Interval:	45m
Offset:	22.5m
Source point interval:	45m
Source line interval:	360m
Full Fold:	84
Fold In-line:	14
Fold Cross-line:	6
Source Parameters	
Source Type:	Dynamite
Charge:	10 kg or 4*2 kg
Hole:	single or 4 pattern
Depth:	15 m or 4m

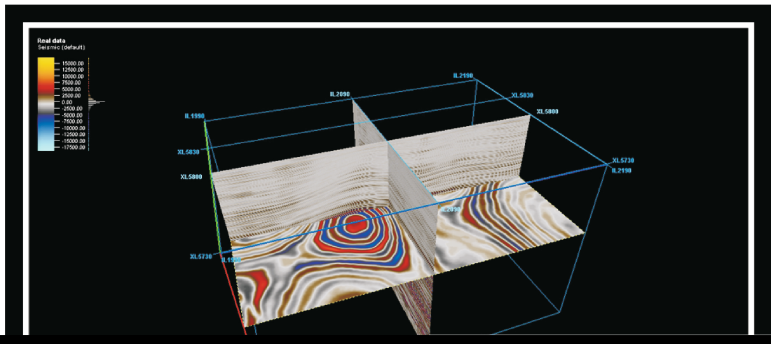
Real data
Seismic (default)
15000.00
12500.00
10000.00
7500.00
5000.00
2500.00
0.00
-2500.00
-5000.00
-7500.00
-10000.00
-12500.00
-15000.00
-17500.00
IL.1950
IL.2050
IL.2150
XL.5830
XL.5880
XL.6730
IL.2150

As is shown in Fig. 2, the footprint noises appear in linear form on time slice. To attenuate the noise, at first, a time slice of seismic data was transferred from the time domain to frequency domain using the 2D recursive filter, eq. (2), as shown in Fig. 3.

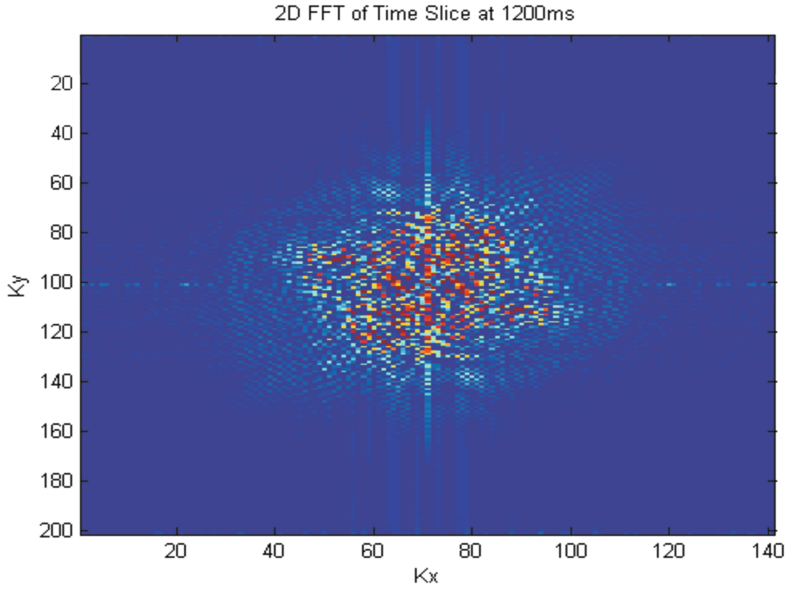

Fig. 3. The Fourier domain transform of the time slice at 1200 milliseconds.

In Fig. 3, the undesirable effects created by the footprint noise are observed along the coordinate axes. The footprints possess higher frequencies comparing to the seismic data. Accordingly, by applying a low pass filter over the frequency domain time-slice seismic data, the footprint noises can be eliminated. The low pass filter allows passing of the low-frequency data, i.e., the seismic data, and hence the high-frequency footprint noises will be attenuated. Fig. 4 shows the 2D cross-section of Fig. 3 after applying the low pass filter.

Comparison of Figs. 3 and 4 indicates that the undesirable effects of the footprint noise with high frequencies are attenuated on the 2D cross-section of the Fourier transformed time-slice. Fig. 5 depicts the time domain representation of Fig. 4.

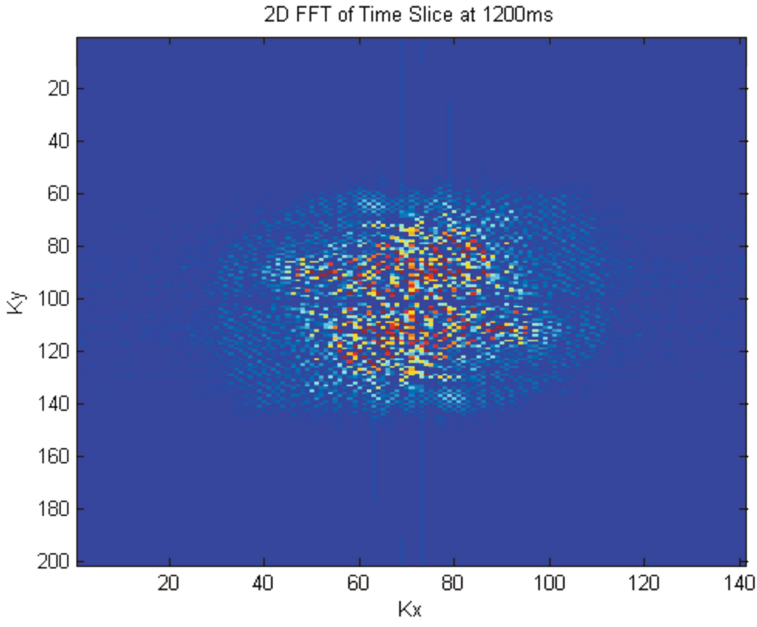

Fig. 4. The two-dimensional cross-section of Fig. 3 after applying the low pass filter.

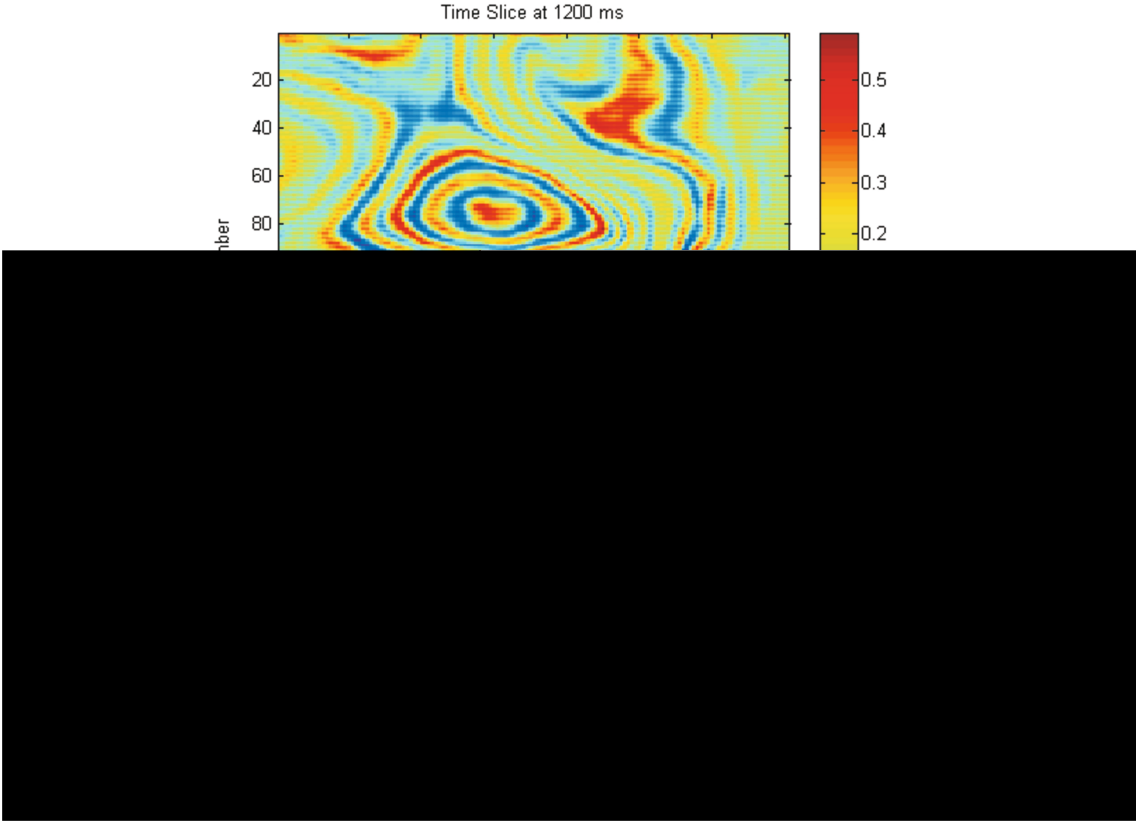

To compare the effect of attenuation with a recursive 2D filter, a time slice at 1200 milliseconds has shown in Fig. 6. The left panel shows the time

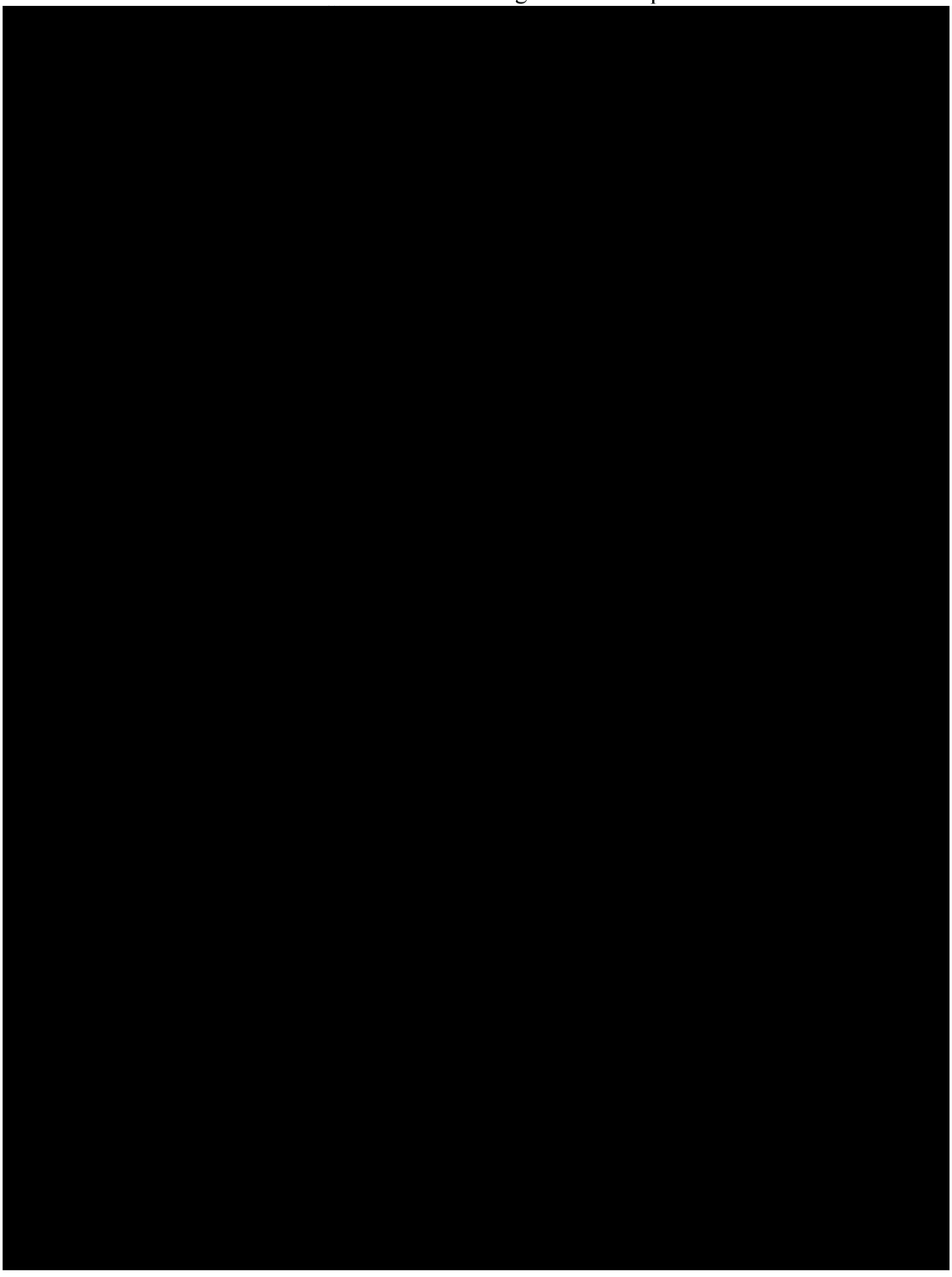

By transforming the time slice to the frequency domain using the 2D recursive filter, applying the low pass filter, and transforming back the frequency domain filtered data to the time domain, the footprints noises can be eliminated. Fig. 8 indicates the filtered time horizon corresponding to 800 ms.

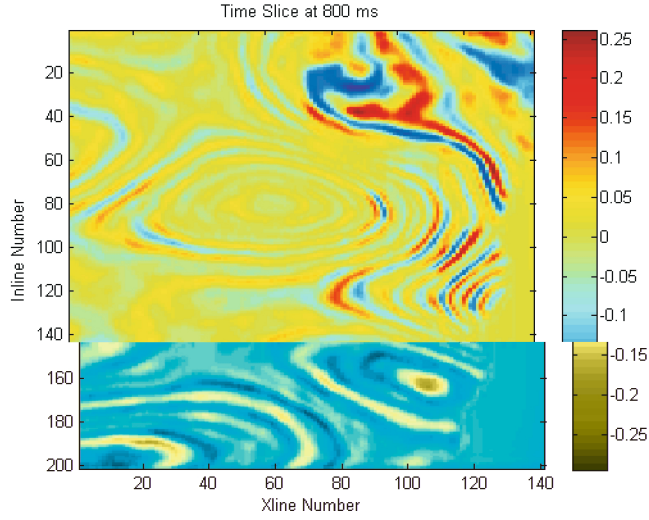

Fig. 8. The filtered footprint-free time horizon corresponding to 800 ms.

As can be seen in Fig. 8, the footprints noises have been significantly attenuated over the time slice of 800 milliseconds. To compare the effect of attenuation using the 2D recursive filter, a time slice at 800 milliseconds in time domain before applying the 2D recursive filter (left panel) and after applying the 2D recursive filter (left panel) are illustrated in Fig. 9.

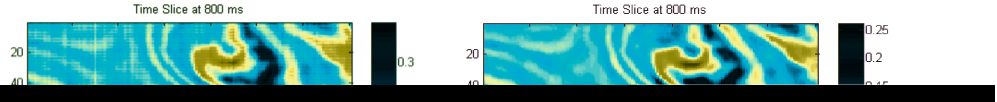

Furthermore, the same procedure is applied again on the time-slice at 1200 milliseconds. Fig. 10 illustrates the 1200 millisecond time-slice over which the footprint noises are observable.

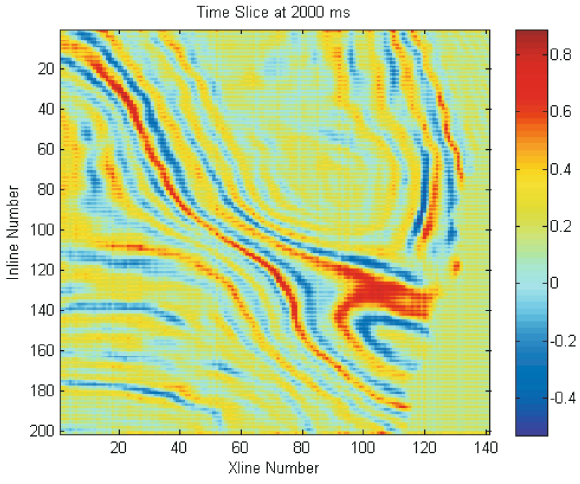

Fig. 10. The time slice at 2000 milliseconds in the time domain and the linear events are the footprint noises.

After transforming from the time-space to the 2D recursive filter space and applying the low pass filter and transforming back the filtered data to the time domain, the footprints are attenuated and the result is depicted in Fig. 11.

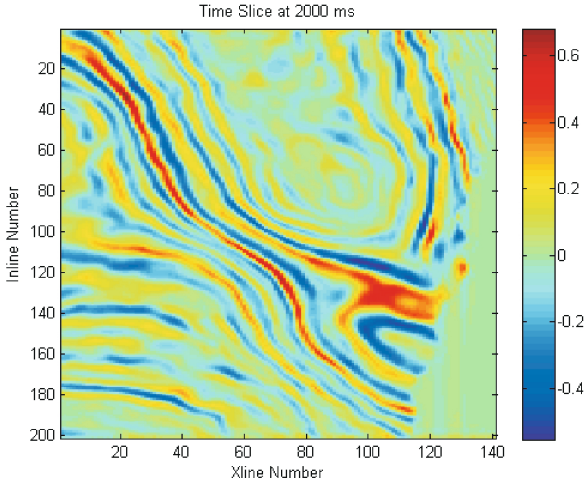

Fig. 11. The time-slice at 2000 milliseconds after applying the 2D recursive filter and using a low pass filter. The attenuation of footprint noises in the time domain is apparent.

As can be seen, the footprint noises have been suppressed for the 2000 millisecond cross section (Fig. 11). To compare the effect of the attenuation using the 2D recursive filter, a 2000 millisecond time-slice before and after applying the 2D recursive filter is shown in Fig. 12.

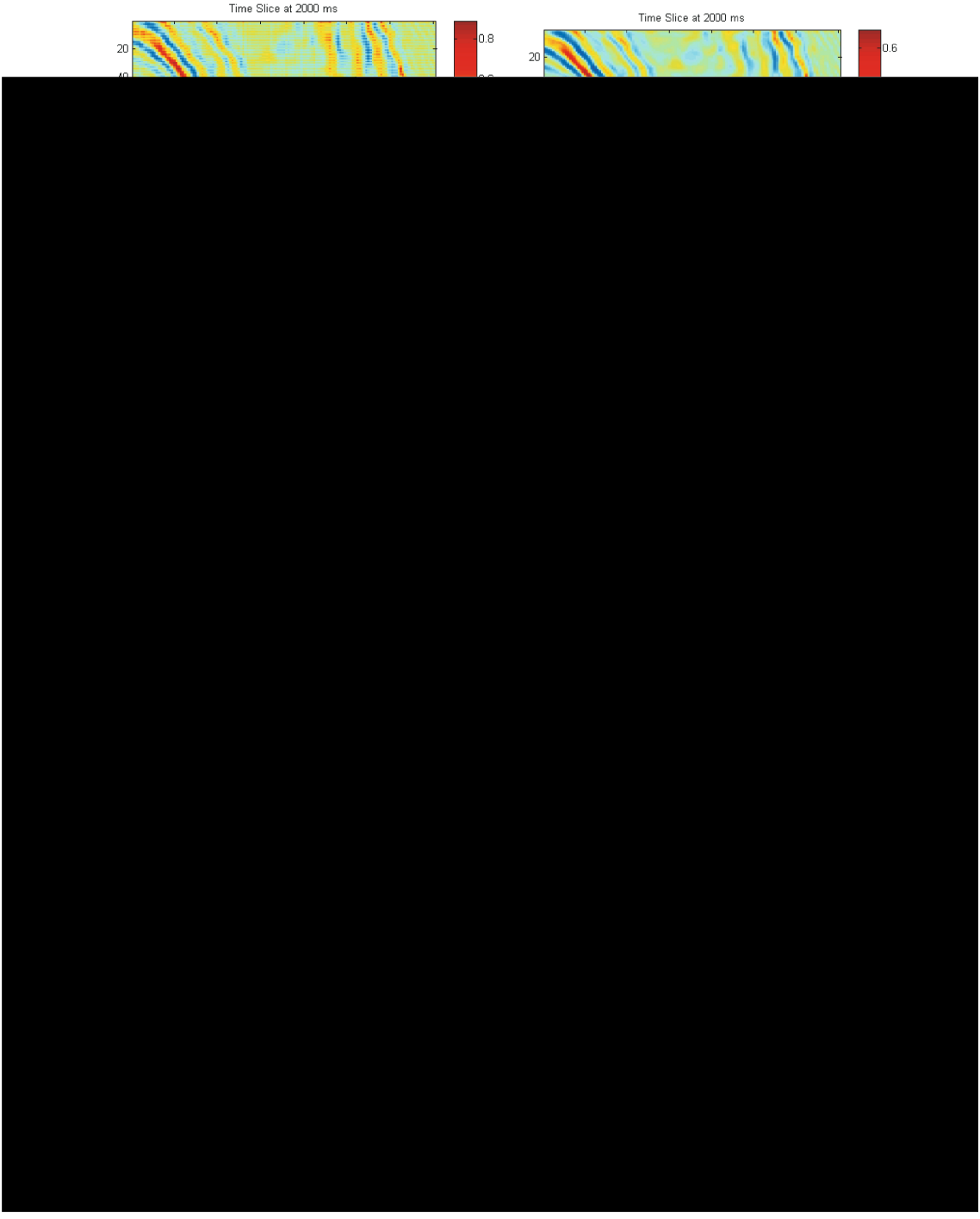

REFERENCES

Alali, A., Machado, G. and Marfurt, K.J., 2016. Attribute-assisted footprint suppression using a 2D continuous wavelet transform. Expanded Abstr., 86th Ann. Internat. SEG Mtg., Dallas: 1898-1902. https://doi.org/10.1190/segam2016-13971687.1.

Al-Bannagi, M.S., Fang, K., Kelamis, P.G. and Douglass, G.S., 2005. Acquisition footprint suppression via the truncated SVD technique. Expanded Abstr., 75th Ann. Internat. SEG Mtg., Houston. https://doi.org/10.1190/1.2032259.

Ben-Zion, Y., Vernon, F.L., Ozakin, Y., Zigone, D., Ross, Z.E., Meng, H., White, M., Reyes, J., Hollis, D. and Barklage, M., 2015. Basic data features and results from a spatially dense seismic array on the San Jacinto fault zone. Geophys. J. Internat., 202: 370-380. https://doi.org/10.1093/gji/ggv142.

Cooley, J.W. and Tukey, J.W., 1965. An algorithm for the machine computation of complex Fourier series. Math. Comput., 19: 297-301.

Drummond, J.M., Budd, A.J. and Ryan, J.W., 2000. Adapting to noisy 3D data-attenuating the acquisition footprint. Expanded Abstr., 70th Ann. Internat. SEG Mtg., Calgary, AB. https://doi.org/10.1190/1.1816247.

de Groot-Hedlin, C.D. and Hedlin, M.A., 2015. A method for detecting and locating geophysical events using groups of arrays. Geophys. J. Internat., 203: 960-971. https://doi.org/10.1093/gji/ggv345.

Gibbons, S.J. and Ringdal, F., 2006. The detection of low magnitude seismic events using array-based waveform correlation, Geophys. J. Internat., 165: 149-166. https://doi.org/10.1111/j.1365-246X.2006.02865.x.

Gulunay, N., 1999. Acquisition geometry footprints removal. Expanded Abstr., 69th Ann. Internat. SEG Mtg., Houston. https://doi.org/10.1190/1.1821103.

Gulunay, N., Benjamin, N. and Magesan, M., 2006. Acquisition footprint suppression on 3D land surveys. First break, 24(2): 71-77.

Inbal, A., Ampuero, J.P. and Clayton, R.W., 2016. Localized seismic deformation in the upper mantle revealed by dense seismic arrays. Science, 354(6308): 88-92. https://doi.org/10.1126/science.aaf1370.

Karagül, A. and Crawford, R., 2003. Use of recent advances in 3D land processing - a case history from the Pakistan Basin area. Extended Abstr., 65th EAGE Conf., Stavanger.

Li, Z., Peng, Z., Meng, X., Inbal, A., Xie, Y., Hollis, D. and Ampuero, J.P., 2015. Matched filter detection of microseismicity in Long Beach with a 5200-station dense array. Expanded Abstr., 85th Ann. Internat. SEG Mtg., New Orleans. https://doi.org/10.1190/segam2015-5924260.1.

Li, Z. and Yao, D., 2016. Microseismic event detection and location using local coherence and subarray beamforming: applications to the Long Beach 3D array and the Hi-CLIMB linear array. Abstr., AGU Fall Mtg., San Francisco.

Marfurt, K.J., Scheet, R.M., Sharp, J.A. and Harper, M.G., 1998. Suppression of the acquisition footprint for seismic sequence attribute mapping. Geophysics, 63: 1024-1035. https://doi.org/10.1190/1.1444380.

Meunier, J. and Belissent, R., 1993. Reduction of 3D Geometry-Generated Artifacts, 3rd Internat. Congr. Brazil. Geophys. Soc., Rio de Janeiro.

Pupeikis, R., 2015. Revised 2D fast Fourier transform. IEEE Open Conf., Vilnius: 1-4. https://doi.org/10.1109/eStream.2015.7119497.

Riahi, N. and Gerstoft, P., 2015. The seismic traffic footprint: Tracking trains, aircraft, and cars seismically. Geophys. Res. Lett., 42: 2674-2681. https://doi.org/10.1002/2015GL063558.

Riahi, N. and Gerstoft, P., 2016. Using graph clustering to locate sources within a dense sensor array. Sign. Process., 132: 110-120. https://doi.org/10.1016/j.sigpro.2016.10.001.

Rost, S. and Thomas, C., 2002. Array seismology: Methods and applications. Rev. Geophys., 40(3): 1008, 2-1–2-27. https://doi.org/10.1029/2000RG000100.

Sahai, S.K. and Sufi, K.A., 2006. Use of simple 2-D filters to reduce footprint noise in seismic data. Geohoriz., 7: 14-17.

Soleymani, H.R., Nejati, M., Arabshahi, S.M. and Riahi, M.A., 2010. Complex trace transformation and its application to suppress random noise. Extended Abstr., 72nd EAGE Conf., Barcelona.

Soubaras, R., 2002. Attenuation of acquisition footprint for non-orthogonal 3D geometries. Extended Abstr., 64th EAGE Conf., Florence.

APPENDIX

```
function [Faf] = frft2(f,a)
% The fast Fractional Fourier Transform
% input: f = samples of the signal
%        a = fractional power
% output: Faf = fast Fractional Fourier transform

% error(nargchk(2, 2, nargin));

f0 = f(:);
N = length(f);
shft = rem((0:N-1)+fix(N/2),N)+1;
sN = sqrt(N);
a = mod(a,4);

% do special cases
if (a==0), Faf = f0; return; end;
if (a==2), Faf = flipud(f0); return; end;
if (a==1), Faf(shft,1) = fft(f0(shft))/sN; return; end
if (a==3), Faf(shft,1) = ifft(f0(shft))*sN;return; end

% reduce to interval 0.5 < a < 1.5
if (a>2.0), a = a-2; f0 = flipud(f0); end
if (a>1.5), a = a-1; f0(shft,1) = fft(f0(shft))/sN; end
if (a<0.5), a = a+1; f0(shft,1) = ifft(f0(shft))*sN; end

% precompute some parameters
alpha=a*pi/2;
s = pi/(N+1)/sin(alpha)/4;
t = pi/(N+1)*tan(alpha/2)/4;
Cs = sqrt(s/pi)*exp(-i*(1-a)*pi/4);

% sinc interpolation
f1 = fconv(f0,sinc([-(2*N-3):2:(2*N-3)]'/2),1);
f1 = f1(N:2*N-2);

% chirp multiplication
chrp = exp(-i*t*(-N+1:N-1)'.^2);
l0 = chrp(1:2:end); l1=chrp(2:2:end);
f0 = f0.*l0;        f1=f1.*l1;

% chirp convolution
chrp = exp(i*s*[-(2*N-1):(2*N-1)]'.^2);
e1 = chrp(1:2:end);  e0 = chrp(2:2:end);
f0 = fconv(f0,e0,0); f1 = fconv(f1,e1,0);
h0 = ifft(f0+f1);

Faf = Cs*l0.*h0(N:2*N-1);

%%%%%%%%%%%%%%%%%%%%%%%%%%%%%%%%
function z = fconv(x,y,c)
% convolution by fft

N = length([x(:);y(:)])-1;
P = 2^nextpow2(N);
z = fft(x,P) .* fft(y,P);
if c ~= 0,
   z = ifft(z);
   z = z(N:-1:1);
end
```